



Contents lists available at ScienceDirect

## Journal of Volcanology and Geothermal Research

journal homepage: [www.elsevier.com/locate/jvolgeores](http://www.elsevier.com/locate/jvolgeores)

# Phreatomagmatic volcanic hazards where rift-systems meet the sea, a study from Ambae Island, Vanuatu

Károly Németh\*, Shane J. Cronin

*Institute of Natural Resources, Volcanic Risk Solutions, Massey University, PO Box 11 222, Palmerston North, New Zealand*

## ARTICLE INFO

### Article history:

Received 13 February 2008

Accepted 14 August 2008

Available online xxx

### Keywords:

phreatomagmatic  
tuff ring  
tuff cone  
maar  
volcanic island  
basalt  
rift  
scoria  
sideromelane  
accretionary lapilli  
base surge

## ABSTRACT

Ambae Island is a mafic stratovolcano located in the northern Vanuatu volcanic arc and has a NE-SW rift-controlled elongated shape. Several hundred scoria cones and fissure-fed lava fields occur along its long axis. After many decades of quiescence, Ambae Island erupted on the 28th of November 2005, disrupting the lives of its 10,000 inhabitants. Its activity remained focused at the central (crater-lake filled) vent and this is where hazard-assessments were focused. These assessments initially neglected that maars, tephra cones and rings occur at each tip of the island where the eruptive activity occurred <500 and <300 yr B.P. The products of this explosive phreatomagmatic activity are located where the rift axis meets the sea. At the NE edge of the island five tephra rings occur, each comparable in size to those on the summit of Ambae. Along the NE coastline, a near-continuous cliff section exposes an up to 25 m thick succession of near-vent phreatomagmatic tephra units derived from closely spaced vents. This can be subdivided into two major lithofacies associations. The first association represents when the locus of explosions was below sea level and comprises matrix-supported, massive to weakly stratified beds of coarse ash and lapilli. These are dominant in the lowermost part of the sequence and commonly contain coral fragments, indicating that the loci of explosion were located within a reef or coral sediment near the syn-eruptive shoreline. The second type indicate more stable vent conditions and rapidly repeating explosions of high intensity, producing fine-grained tephra with undulatory bedding and cross-lamination as well as megaripple bedforms. These surge and fall beds are more common in the uppermost part of the succession and form a few-m-thick pile. An older tephra succession of similar character occurs below, and buried trees in growth position, as well as those flattened within base surge beds. This implies that the centre of this eruption was very near the coastline. The processes implied by these deposits are amongst the most violent forms of volcanism on this island. In addition, the lowland and coastal areas affected by these events are the most heavily populated. This circumstance is mirrored on many similar volcanic islands, including the nearby SW Pacific examples of Taveuni (Fiji), Upolu and Savai'i (Samoa), and Ambrym (Vanuatu). These locations are paradoxically often considered safe areas during summit/central-vent eruptions, simply because they are farthest from the central sources of ash-fall and lahar hazard. The observations presented here necessitate a revision of this view.

© 2008 Published by Elsevier B.V.

## 1. Introduction

Growing populations on active volcanic islands face complex volcanic hazards (Mattioli et al., 1996; Cole et al., 1999; Arana et al., 2000; Cronin et al., 2001; Cronin and Neall, 2001; Carn et al., 2004; Cronin et al., 2004; Malheiro, 2006). Many of these volcanic islands are dominated by a central volcanic edifice. Hazards from these geographically confined volcanic edifices are relatively easy to comprehend for inhabitants of the islands regardless of their development state (Cronin et al., 2004). Many volcanic islands, however, may have volcanic eruptions not only at their central volcanic zones but along

lateral flank vents, which are often referred to as satellite volcanoes. Some island volcanoes may also have a central volcanic edifice, which doesn't appear to be an actual central vent to lay people such as Taveuni, Fiji (Cronin and Neall, 2001). In these situations, the location of re-awakening activity on the flanks may be difficult to forecast (Cronin et al., 2001). Flank eruptions on these structures are commonly complex, involving multiple eruption phases, rejuvenation, and complex sources. Their distributional pattern largely depends on the structural architecture, and can range from single elongated rift zones (e.g. Taveuni, Fiji) to broad and poorly defined rift structures (e.g., Savai'i, Samoa) and more evenly scattered volcanic edifices around a central vent (e.g., Jeju, South Korea). Prediction and probabilistic volcanic hazard assessment is simpler in single-rift axis volcanic fields, but where central volcanoes exist, hazard assessment is commonly concentrated upon them at the expense of flank features. Logistical

\* Corresponding author.

E-mail address: [k.nemeth@massey.ac.nz](mailto:k.nemeth@massey.ac.nz) (K. Németh).

difficulties stand in the way of obtaining sufficient age, chemical, or stratigraphical data to establish a refined volcanic stratigraphy in these flank regions. As a result, hazard assessments for a volcanic island can be very focused on the central vent system. In some cases these structures may pose the greatest threat to the island. However, in other cases flank eruptions may be of a comparable size and hazard potential.

Volcanic islands have complex structures, similar to stratovolcanoes, comprising coherent (effusive and intrusive) and clastic volcanic rocks with variable degrees of alteration, weathering and thickness variations, thus resulting in unique hydrogeology (Boubekraoui et al., 1998; Violette et al., 2001; Join et al., 2005). Moreover, being surrounded by sea influences their hydrogeology as well as the entire gravitational stability of the growing volcanic edifice (Carracedo et al., 1999; Day et al., 1999; Walter et al., 2005; Munn et al., 2006).

In this study we concentrate on eruptions that pose hazard particularly in the coastal areas of a volcanic island. Eruptions along coastal areas commonly involve phreatomagmatic eruptions as a

result of the water saturation of the sediments in the coastal plains, or within the surrounding shallow seas of the islands. This fact and the growing coastal population of volcanic islands make these coastal or near-shore eruptions potentially dangerous. Attention is particularly highlighted on the locations where major rift axes meet the sea, where the eruptions are most likely to be concentrated. In this paper we document apparently young volcanic landforms and deposits forming the northeastern edge of the volcanic island of Ambae (Aoba) in Vanuatu (New Hebrides). These structures are interpreted in relation to similar features in other SW Pacific volcanic islands and are used to assess the degree of hazard posed by the rift-edge volcanism.

## 2. Geological setting

Ambae (Aoba) is part of the Vanuatu active volcanic arc located in the northern-central part of the archipelago (Fig. 1A). The NE-SW elongated island has a characteristic rift zone that has an en-echelon

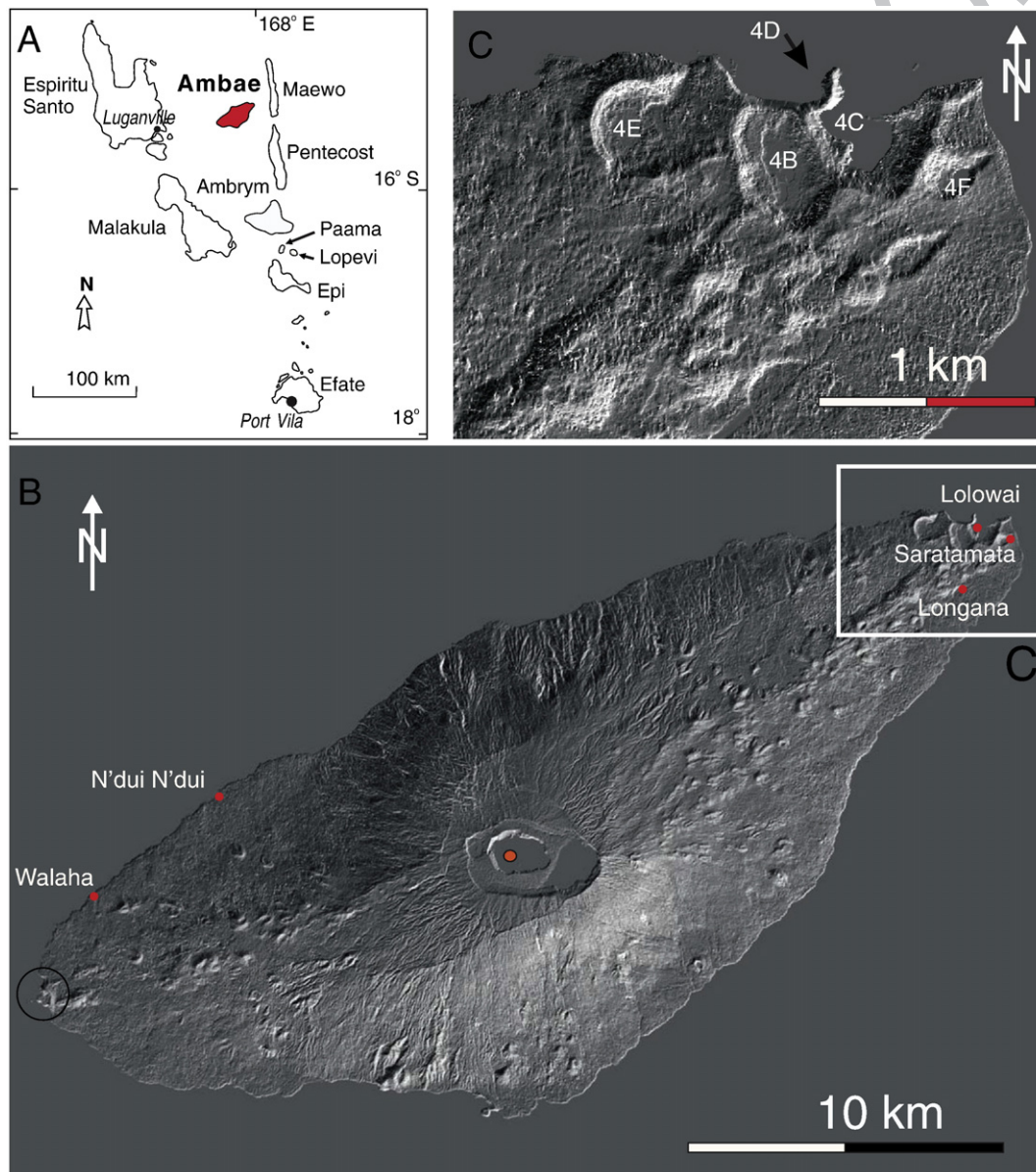


**Fig. 1.** A) Location of Ambae Island, part of the Vanuatu archipelago. B) Digital elevation model of Ambae Island shows well-developed rift axis dotted with scoria cones. The central vent complex with a caldera lake (Lake Vui) confined in a large tuff ring was a place of past intra-caldera Surtseyan-style explosive eruptions such as the 2005 December eruption. N'dui N'dui village and its surrounding area is mentioned in oral traditions as a site of the AD 1670 lahar disaster. Saratamata and Longana (in white box) are the two villages where human occupation sites were identified embedded in distal scoria fall and phreatomagmatic tephra. C) An enlargement of the NE rift-edge area of Ambae where half sections of phreatomagmatic volcanoes (numbers) form a volcanic field. Numbers refer to the views shown on Fig. 4.

97 offset structure on each side of the central vent system (Fig. 1B). This  
 98 complication to the rift system is related to the cross-arc stresses  
 99 caused by the subduction of a slab of continental crust (the Louisville  
 100 Ridge) beneath the central volcanic arc (Meffre and Crawford, 2001;  
 101 Calmant et al., 2003). The rift system forms an incipient graben  
 102 structure with scoria cones, lava spatter cones and lava flows within  
 103 and concentrated along its margins. These form a volcanic ridge  
 104 developed upon a basaltic (pyroxene, olivine and picritic) lava shield  
 105 (Fig. 1B). Ambae emerges up to 1496 m above sea level, culminating in  
 106 the Lombenben Volcano (Mount Manaro) (Fig. 1B). Overall, Ambae is  
 107 the most voluminous active volcanic island in the Vanuatu archipe-  
 108 lago (Fig. 1A) with the summit standing 3900 m above the  
 109 surrounding seafloor. The central part of the island forms a nested  
 110 caldera system (Warden, 1967; Warden, 1970). Two distinct caldera  
 111 structures (Fig. 1B) occur with the floor presently about 150 m deep  
 112 (Warden, 1967; Warden, 1970). The age and the origin of the caldera  
 113 are unknown, although the lack of a widespread evolved pyroclastic  
 114 succession on the island suggests it formed through gradual sub-  
 115 sidence, possibly driven by lateral drainage of the magmatic plumbing

system through a flank dyke system (Warden, 1970). The caldera  
 116 complex is occupied by a large phreatomagmatic tephra ring enclosing  
 117 the 2.3-km-diameter acidic (pH 1.8) Lake Vui (Fig. 1B) (Warden, 1970;  
 118 Garaebiti, 2000). This body of water is one of the major concerns in  
 119 any volcanic hazard assessment on Ambae (Fig. 2) due to its potential  
 120 for lahar generation in the case of large explosive eruptions through  
 121 the lake (Cronin et al., 2004). The eruptive history of Ambae following  
 122 its emergence from the sea about 0.7 million years ago (Warden, 1970)  
 123 is unknown. Warden (1970) inferred that the central tuff ring and Lake  
 124 Vui were probably formed during eruptions around 1575 accompa-  
 125 nished with lava flow effusion in the northern slopes. Extensive lava  
 126 flows reported from traditional stories are inferred to have destroyed  
 127 N'dui N'dui village around 1670 on the western flanks of the island.  
 128 Lahar-triggering eruptions are also inferred from traditional stories  
 129 during an eruption in 1870. Lahars initiated by landslides probably  
 130 due to an eruption were reported from 1914. In both lahar events,  
 131 villages were destroyed with many fatalities (de la Rüe, 1956; Blot and  
 132 Priam, 1962; Williams and Warden, 1964). Since then, many small-  
 133 scale phreatic and gas-release events have occurred from Lake Vui  
 134

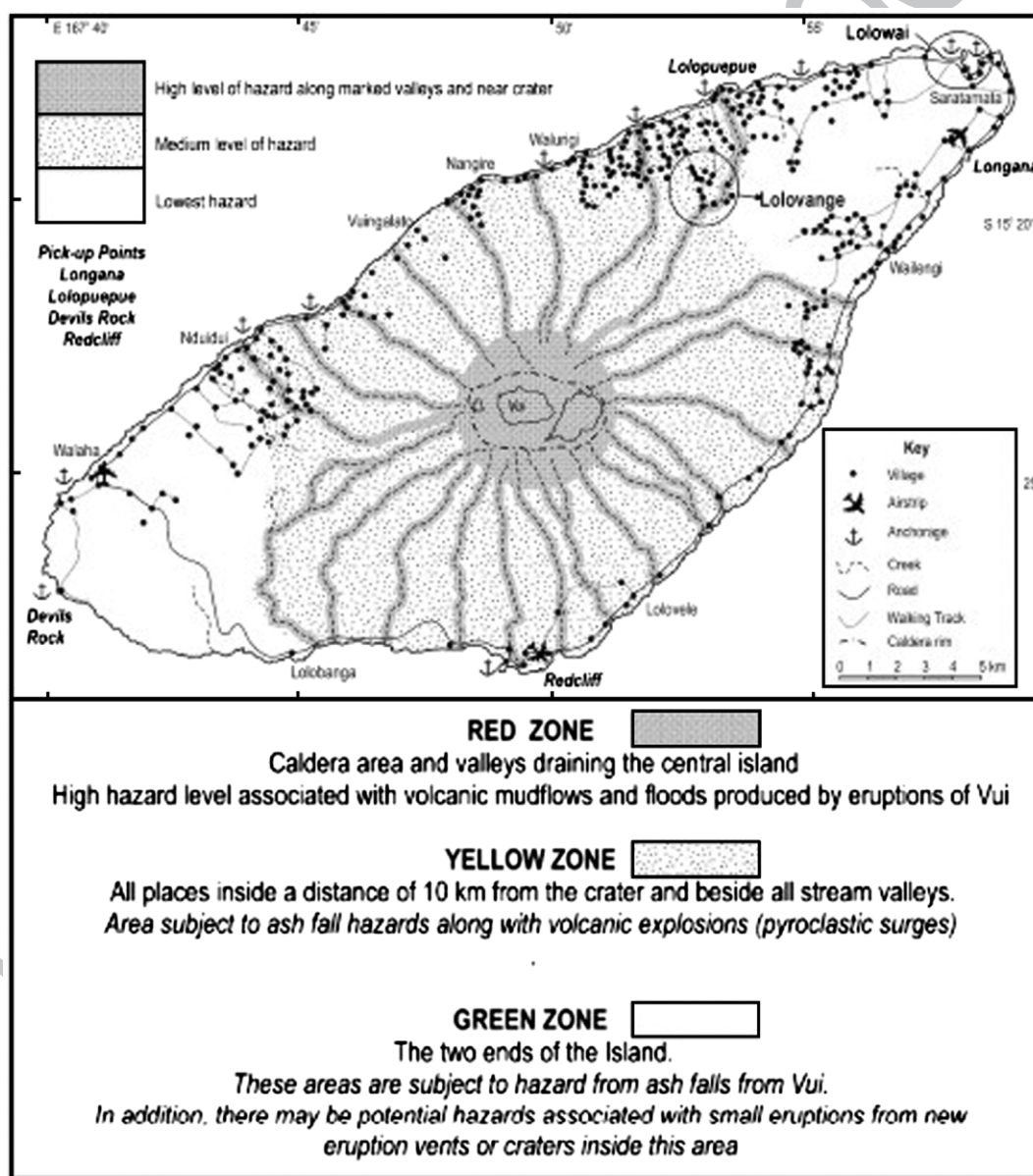


Fig. 2. An English version of the current volcanic hazard map of Ambae (after Cronin et al., 2004). The main colour zones predominantly reflect the main volcanic hazards associated with eruption triggered lahars from the summit vents.

with acid rain and small explosions in 1995. This event caused significant alarm on the island along with calls for partial evacuation (Robin et al., 1995). In 2005 December, Ambae had a fully developed intra-caldera Surtseyan-style eruption forming a tuff cone in the caldera lake (Németh et al., 2006). In spite of the general view that lahars were initiated from the central caldera lakes by volcanic eruptions (Garaebiti, 2000) as well as traditional stories (Cronin et al., 2004), no convincing evidence of major widespread lahar deposits have been described so far in the major tributaries surrounding the central caldera (Fig. 2). A volcanic hazard map (Cronin et al., 2004) and associated exclusion zones are based primarily on central-vent events (Fig. 2). Large-scale eruptions are last known from Ambae several generations ago (Cronin et al., 2004). However, island inhabitants are reminded of its volcanic origin by periodic eruptions through Lake Vui, including the most recent surtseyan episode of December, 2005 (Fig. 3) (Németh et al., 2006). The four weeks of surtseyan activity formed a 100 m high tephra cone, up to 250 m across. The same scenario occurred in 1870 (Warden, 1970). Phreatic eruptions occurred in 1966 and 1995 (Lardy et al., 1997). Apart from these events, however, the eruption chronology and stratigraphy of the island is largely unknown. Therefore, no reliable data can be used to interpret any connection between central and rift-axis eruptions. The last known rift volcanism is a major lava field formation in the N'dui N'dui area (Warden, 1970; Cronin et al., 2004, 2008). In addition, fresh morphology of several scoria cones suggests Holocene volcanism.

At the terminations of the rift in both sides of the island, large tuff rings are the main volcanic landforms (Fig. 1B). On the SW coast, a half section of a tuff ring forms an embayment (Fig. 1B) while in the NE a complex group of 5 tuff rings are clustered (Fig. 1C). The size and architecture of these tuff rings are comparable to the central intra-caldera tuff ring.

### 3. Morphology of rift-edge phreatomagmatic volcanoes

The geometry of the structures (broad crater, low crater rim and gently dipping pyroclastic units) indicates that the volcanic landforms in the NE side of Ambae are tuff rings similar to those identified in the coastal areas of Jeju Island (Korea) (Sohn, 1996). However, the original

morphology of these volcanic landforms is modified and their preserved volcanic successions are rather thick compared with the Korean examples. They likely represent transitional landforms between tuff rings and fully developed tuff cones.

In addition to the 5 on-shore tuff rings (Fig. 4A), the northern coastline morphology indicates that another structure is located just offshore (Fig. 1C). Under their heavy tropical vegetation cover (Fig. 4B), their morphology is extremely fresh (Fig. 1C). The young ages of these tuff rings are confirmed by local legends and traditional knowledge of village communities (Cronin et al., 2004). The preserved crater diameters range from about 250 m to 1500 m across, with rims up to 100 m high. The crater floors are flat and filled with swamps and shallow lakes (Fig. 4B), and the inner crater rim is marked by steep, sub-vertical cliffs mantled with colluvium. No characteristic gully networks occur on the cones. Two are breached by the sea and form bays (Fig. 4C, D), either dry (Fig. 4E) or containing a lake (Fig. 4D). The tuff rings are used for public grounds of a large school and a regional hospital (Fig. 4E) or as fresh-water reservoirs (Fig. 4F). The deposits of the tuff rings are overlapping and their close spacing suggests some were formed in a relatively short period of time. It is not sure whether these are stand-alone eruption sites or whether they were derived from magmas drained through lateral dyke systems similar to the phreatomagmatic rift-edge volcanic fields in the nearby Ambrym Island about 30 km to the south where at least 7 phreatomagmatic volcanoes were formed in 1913 following a central vent eruption in the summit of Ambrym (Frater, 1917; Gregory, 1917; Robin et al., 1993; Németh and Cronin, 2007).

### 4. Pyroclastic successions of phreatomagmatic volcanoes

Pyroclastic successions of the tuff rings in the NE edge of the island crop out along the shoreline and along a road cut. These outcrops give data about the lateral extent of the tephra associated with the explosive eruption of the monogenetic volcanoes in the rift edge. They will be described following the full description of the half sections of the proximal, cone-building pyroclastic units.

In the road cuts, pyroclastic sequences of the tuff ring 4B (on Figs. 1C and 4B) are exposed, while the northern coastline comprises a



Fig. 3. Intra-caldera Surtseyan-style explosive eruption in December 2005 built a tuff cone in the caldera lake.

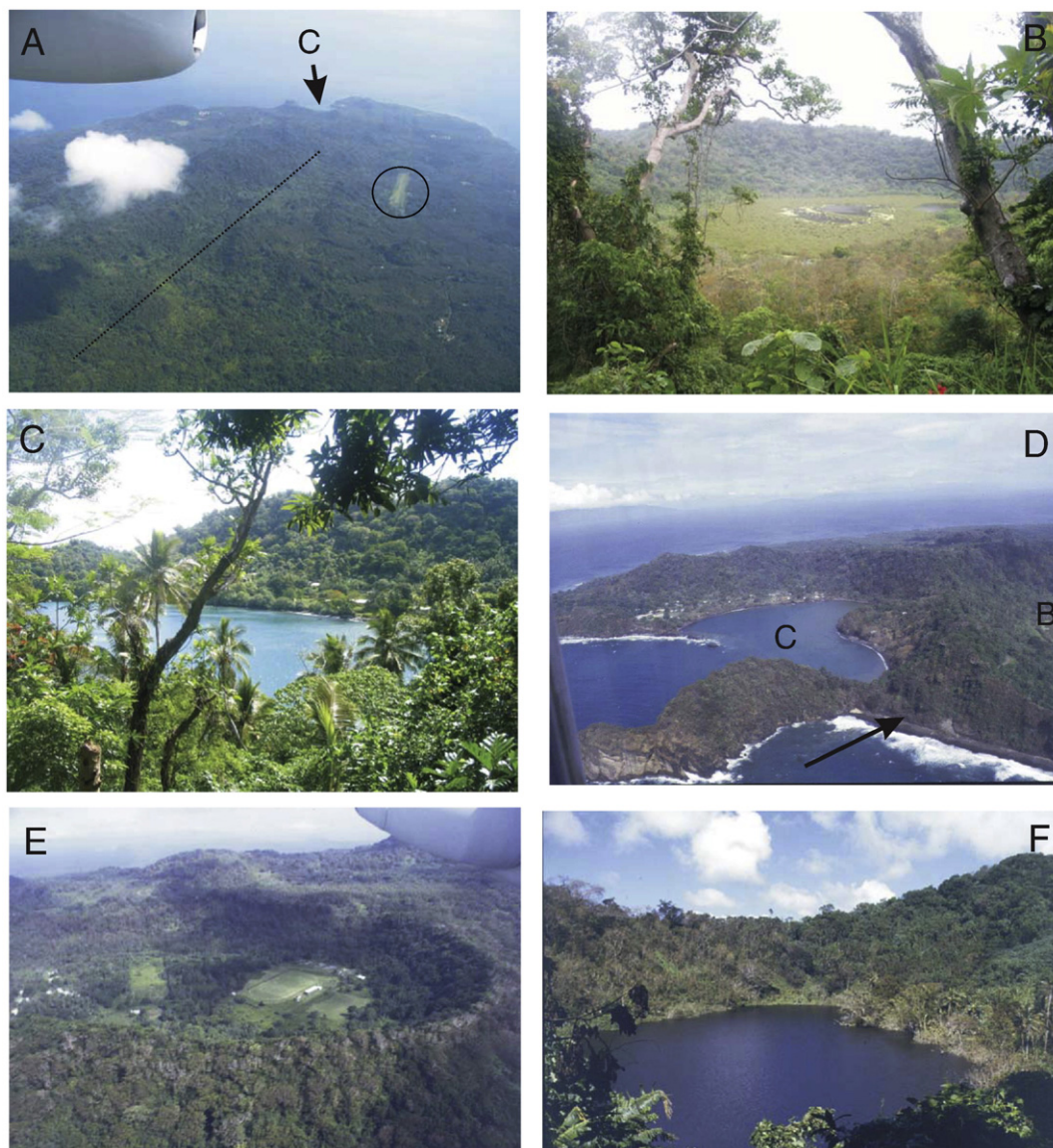


**Fig. 4.** Phreatomagmatic volcanoes from NE Ambae demonstrate a great variety of sizes and preservation conditions. On "A" dotted line marks the approximate position of the rift axes. The airfield is circled. The view numbers are shown on Fig. 1C. On "B" the crater is occupied by a swamp. On "C" and "D" a phreatomagmatic volcano is shown with breached crater rim that gave way to enter the sea. According to local legends (e.g. Cronin et al., 2004) before the sea gained access to the crater it was filled with fresh water lake, similar to another phreatomagmatic volcano shown on "F". A school perfectly set in the dry crater of the westernmost phreatomagmatic volcano (E).

207 near-continuous proximal-to-distal sequence of phreatomagmatic  
 208 deposits that can be traced as part of the 4C tuff ring (on Figs. 1C  
 209 and 4C). The base of the 4C sequence is separated by an immature soil  
 210 horizon from an older sequence of phreatomagmatic deposits  
 211 apparently sourced from an offshore vent site (Fig. 5B and C). There  
 212 is no outcrop from the otherwise morphologically well-preserved  
 213 4E or 4F tuff rings (on Figs. 1C, 4 E, and F). Along some of the road  
 214 sections, textural differences between the upper pyroclastic units  
 215 show two different source vents, the 4B and 4C craters (Fig. 5D). The  
 216 exposed pyroclastic units are fairly monotonous and can be distin-  
 217 guished into 4 major lithofacies. The volumetrically dominant  
 218 lithofacies is a well bedded, thinly cross-bedded, poorly sorted tuff  
 219 with common ripple and mega-ripple features (L1). This makes up  
 220 approximately 60% of the exposed pyroclastic units. The L1 lithofacies  
 221 is interbedded with unsorted lapilli tuff composed of 10 cm-thick  
 222 individual units showing slightly undulating bedding planes (L2). The  
 223 L2 lithofacies comprises c. 20% of the volume. In the proximal areas of  
 224 the 4C tuff ring, volcanic-lithic rich bomb and block horizons form a  
 225 tuff breccia (L3) that can be traced along the coastal exposures. This

lithofacies comprises about 15% of the total volume of exposed 226  
 deposits. Scoriaceous lapilli beds with uniform bed thickness and 227  
 parallel bedding planes (L4) can be identified sporadically throughout 228  
 the exposed cliffs. This lithofacies comprises about 5% of the total 229  
 volume of the exposed pyroclastic units. Along the coastline exposures 230  
 the proportion of L3 lithofacies is larger in the proximal areas of the 4C 231  
 phreatomagmatic volcano. In distal areas about 1 km away from the 232  
 4C tuff ring, the proportions of L1 and L2 lithofacies gradually increase. 233

## 5. L1 lithofacies 234

### 5.1. Description 235

L1 lithofacies consists of fine-grained tuff and minor lapilli tuff 236  
 (Fig. 6A). It is thin-bedded with sharp and undulating bedding planes. 237  
 The pyroclastic deposits are poorly sorted and dominated by angular, 238  
 moderately altered, glassy pyroclasts. Thin ash coating on lapilli frag- 239  
 ments is common with thin palagonite rims on juvenile fragments. 240  
 The juvenile fragments constitute c. 70% of the clasts. The remainder 241



**Fig. 5.** Half section of a phreatomagmatic volcano in the northern coastline (A). Numbers on “A” refer to the detailed textural photos shown on Fig. 7D and C. People are for scale in circle. On “B” the complex stratigraphy (letters are lithofacies names) is shown with an interbedded soil horizon (dotted line marks its top). Standing tree remains are in circle. A close up view shows (on “C”) the immature soil horizon (U) separate two major eruptive units. Thin arrows mark a tree remain moved by the pyroclastic density currents (inferred transport direction is marked by a thick arrow). Other tree branch remains marked with circles. On “D” the proximal tuff ring section is shown where sea water gained access to the crater. Dashed line mark the projection of the relatively low dipping pyroclastic units.

of the of grains are ash-sized and predominantly microcrystalline basalt fragments and subordinately coral or beach sand. Strongly palagonitized, rounded lapilli tuff clasts occur occasionally. The L1 lithofacies in coastal exposures becomes dominant with increasing distance from the proximal part of the 4C tuff cone (Fig. 6A). L1 contains well-developed mega-ripples with wavelengths of 0.1 to 2 m (Fig. 6A) and amplitudes of up to 1 m (Fig. 6B). In the middle section of the coastal cliffs, a persistent horizon of mega-ripples can be traced over tens of metres (Fig. 6A). This lithofacies also contains rim-type accretionary lapilli in tuff beds that commonly mantle ripples. Mantling fine-grained tuff beds have low density and contain abundant fine vesicles.

## 5.2. Interpretation

Beds of L1 lithofacies are interpreted to be deposited from horizontally moving pyroclastic density currents, such as base surges, as shown by mega-ripple bedforms, cross-bedding and common inverse-to-normal grading (Moore, 1967; Fisher and Waters, 1970; Waters and Fisher, 1971; Wohletz and Sheridan, 1979; Chough and Sohn, 1990; Lajoie et al., 1992; Dellino et al., 2004b). The poor sorting and common grain size changes at bed boundaries also suggest deposition from pyroclastic density currents (White and Schmincke, 1999; Dellino and La Volpe, 2000; Gladstone and Sparks, 2002; Gurioli et al., 2002; Scolamacchia and Macias, 2005; Sulpizio et al., 2007). The fine-grained nature and non-cohesive texture of the individual beds suggest low particle concentrations and turbulence of the pyroclastic density currents (Yamamoto et al., 1999; Dellino et al., 2004a; Dellino et al., 2004b). The plastering effect upon large clasts also supports deposition from of a PDC (Vazquez and Ort, 2006; Lorenz, 2007). The

abundance of rim-type accretionary lapilli (Schumacher and Schmincke, 1991; Schumacher and Schmincke, 1995), especially in the more distal areas, indicates high moisture contents but not water saturation in the base surges. This is also supported by the general lack of post-depositional soft-sediment deformation structures such as dewatering structures and slumping surfaces, which are expected in wet surge deposits (Dellino et al., 1990). The flow indicators (Bogaard and Schmincke, 1984) exclusively suggest a unidirectional transport from the east, i.e., the presumed vent location of the 4C phreatomagmatic volcano, which is at present submerged by breaching of its northern rim by wave action. The thin mantle-bedded layers over ripples suggest fallout from co-surge ash cloud after a series of pyroclastic density currents passed the depositional sites (Dellino et al., 2004a; Vazquez and Ort, 2006). The abundance of accidental lithic fragments suggests that the exposed sites along the shoreline are part of a phreatomagmatic volcano in which eruption the excavation of country rock fragments played an important role in the formation of the volcanic edifice (Godchaux et al., 1992; Aranda-Gomez and Luhr, 1996; Martin and Németh, 2005). Low-density, vesicle-rich tuff beds interpreted to be vesiculated (vesicular) tuffs are a result of entrapment of air and condensing steam in the fine tephra as it has been documented in many phreatomagmatic volcanoes worldwide (Lorenz, 1974b).

## 6. L2 lithofacies

### 6.1. Description

L2 is a stratified, weakly to moderately bedded lapilli tuff (L2a) and tuff (L2b) lithofacies. This lithofacies dominates the proximal areas of

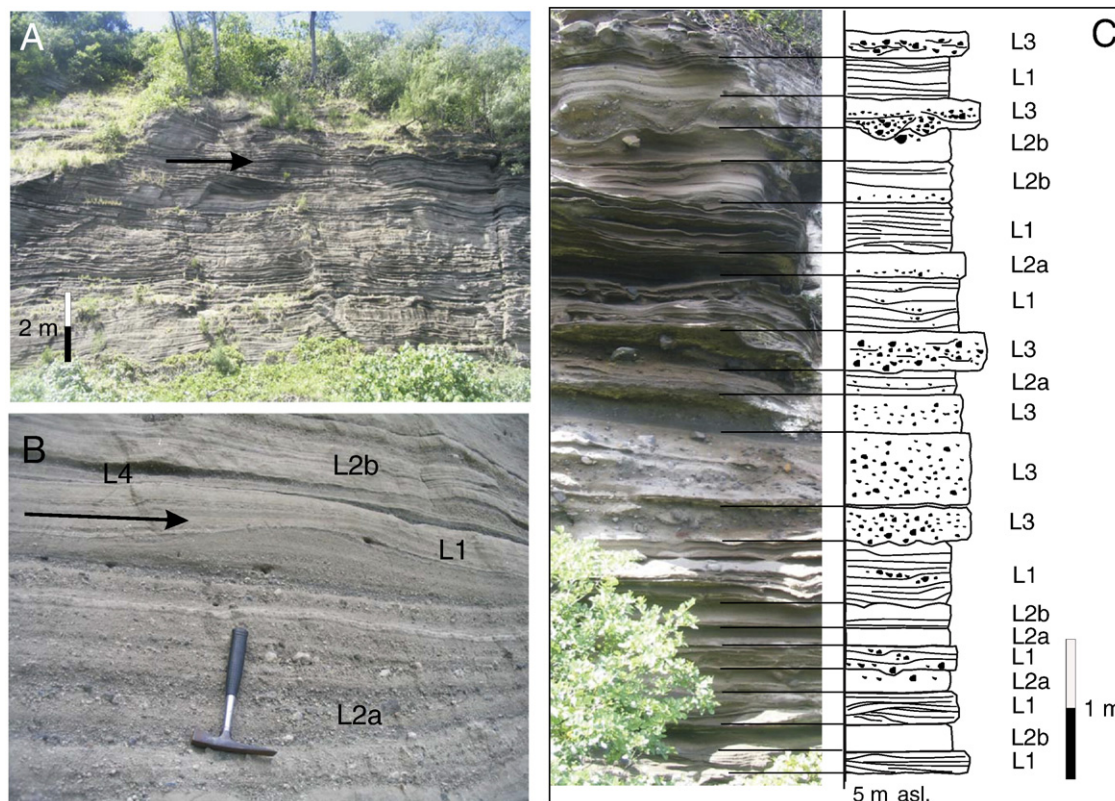


**Fig. 6.** Pyroclastic density current dominated succession in medial section (A). Inferred transportation direction is marked by the arrow. Close up view (B) of a dune in the pyroclastic density current succession indicating left to right transportation (arrow). Simplified stratigraphy log of the proximal pyroclastic successions (C) shows the distribution pattern of identified lithofacies. Lithofacies codes are explained in the text.

the 4C tuff cone (Fig. 6C), although beds become finer (i.e., L2b) with increasing distance from the vent over about 500 m. L2 is dominated by angular juvenile ash and lapilli with moderate palagonitisation. The beds have undulating bedding planes, and they are unsorted or inverse-to-normally graded. Inverse grading is more prominent in coarser-grained beds (L2a). About 30 vol.% of L2 is rich in accidental lithic clasts, including different types of coherent basaltic rocks, coral fragments (Fig. 7A) or altered and probably older lapilli tuff fragments (Fig. 7B). The proportion of L2 beds is higher in the eastern side of the coastal outcrops near the presumed vent site of the 4C tuff cone.

## 6.2. Interpretation

The beds of this lithofacies are interpreted to have been deposited from laterally moving pyroclastic density currents such as base surges and pyroclastic flows. The progression from L2 to L1 beds with distance from source is similar to that described in many tuff rings, such as Hopi Butte, Arizona (Vazquez and Ort, 2006), Linosa, Italy (Lajoie et al., 1992), Pinacate, Sonora (Wohletz and Sheridan, 1983; Gutmann, 2002; Martin and Németh, 2006) or many tuff rings from Jeju Island, Korea (Sohn and Chough, 1989; Chough and Sohn, 1990; Sohn, 1996). The lateral facies changes of the L2 lithofacies from coarse- to fine-grained subfacies suggest gradual loss of competence of the pyroclastic density currents. The L2 beds appear to have formed from pyroclastic density currents with high particle concentrations, involving significant excavation of country rock in shallow subsurface explosion sites (Lorenz, 1986). The coarse grain size and abundant country rock fragments from near-surface lithologies indicate stable explosion locus position of individual explosions in the near-surface country rock (e.g. beach platform) and relatively low-efficiency fragmentation itself (Lorenz, 1986; Lorenz and Kurszlauskis, 2007).

## 7. L3 lithofacies

### 7.1. Description

L3 lithofacies is most common in the proximal areas of the 4C phreatomagmatic volcano (Fig. 8A). It forms thickly bedded, accidental-lithic bomb and lapilli-rich units (Fig. 8B). Impact sags are common, penetrating and deforming the underlying finer-grained beds (L1 or L2 beds). In proximal areas the pyroclastic rocks form distinctive and laterally persistent beds (Fig. 8A), while in more distal areas they tend to form single-bomb horizons (or trains) within an unsorted coarse ash matrix (Fig. 8B). In proximal areas individual beds of L3 are up to 1 m thick and comprise matrix-supported unsorted tuff breccias. Within the tuff breccia, lensoidal zones of coarse lapilli are common. Also in the proximal areas, L3 beds commonly exhibit channel-like features with flat tops and U-shaped basal contacts. Accidental lithic clasts include predominantly volcanic lithic fragments with angular to sub-rounded shapes.

### 7.2. Interpretation

The beds of L3 lithofacies are interpreted to have resulted from major vent-clearing explosions that excavated significant volume of country rocks (White, 1989; Büchel and Lorenz, 1993; Mastrolorenzo, 1994; Ort et al., 1998; Vazquez and Ort, 2006). Their massive texture and sheet-like architecture in proximal areas are consistent with deposition from laterally moving high-particle-concentration pyroclastic density currents (Chough and Sohn, 1990; Sohn, 1996). Additional country rock material was apparently added by jet-like explosions (Kokelaar, 1983; Kokelaar, 1986) and entrained by the gravity currents (Dellino et al., 2004a). The coarse-grained lenses in L3

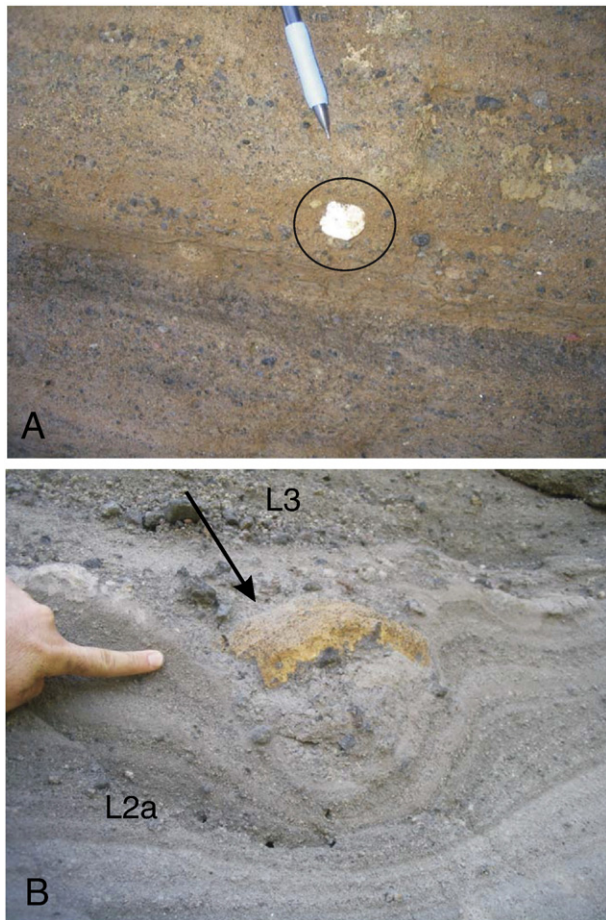


**Fig. 7.** Picked up coral fragments (circle) in a phreatomagmatic pyroclastic rock in distal succession (A). Bomb sag caused by an already diagenised lapilli tuff fragments from an older pyroclastic unit (B). Arrow marks the inferred transportation direction.

could be interpreted as scour-fill features, where passing density currents erode small scours and subsequent currents leave behind lag deposits (Schmincke et al., 1973; Chough and Sohn, 1990). U-shaped channels similar to the channels identified in a few proximal beds of L3 are commonly interpreted to be erosional channels caused by the moving pyroclastic density currents (Crowe and Fisher, 1973; Fisher, 1977). The common association of such U-shaped channels with large lapilli and bomb sized clasts and complex impact features suggests that these features were produced by direct debris jets, similar to those described at “wet” volcanoes associated with emergent volcanism (Leat and Thompson, 1988; Mueller et al., 2000). Other failure mechanisms for forming U shaped channels in wet deposits (Lorenz, 1974a; Sohn and Chough, 1992) are less likely based on the extent and geometry of the channels being closely associated with primary deposits under- and overlaying the channels.

## 8. L4 lithofacies

### 8.1. Description

L4 lithofacies is the least common facies of the exposed pyroclastic succession of the tuff rings however it is common in small outcrops in the inter-cone areas in NE Ambae. It comprises thinly bedded scoriaceous coarse ash and lapilli with better sorting characteristics than the other lithofacies. The beds of L4 are laterally continuous over tens of metres, although thin beds tend to pinch out over a few metres. The scoriaceous ash and lapilli are fresh, angular, and equi-

dimensional. Vesicles are smooth-walled. The scoriaceous ash and lapilli are black with no alteration rims.

### 8.2. Interpretation

L4 represents fall deposits from strombolian-style eruption. The rarity of these beds in the tuff ring units of 4C volcano indicates that phreatomagmatic explosions were dominant during the eruption of the 4C phreatomagmatic volcano. The irregular thicknesses of such beds and their lateral discontinuity indicate that falls were short-lived and may have been generated by brief, unstable lava fountains. Such eruptive scenario is consistent with ascending magma that only rarely pierces a wet vent zone during transient periods of higher magma output rate or through relatively drier parts of the vent zone.

## 9. Distal pyroclastic units

The pyroclastic succession along the northern coast line is inferred to have resulted from at least 3 major eruptive events. A major break between these eruption events is shown by an intercalated soil with plant fragments and fossilised trees, some standing in growth position (Fig. 9A). This suggests a time gap of at least several decades between the two eruptive events. The standing trees preserved in the basal zone of the depositional surface of the second (middle) pyroclastic

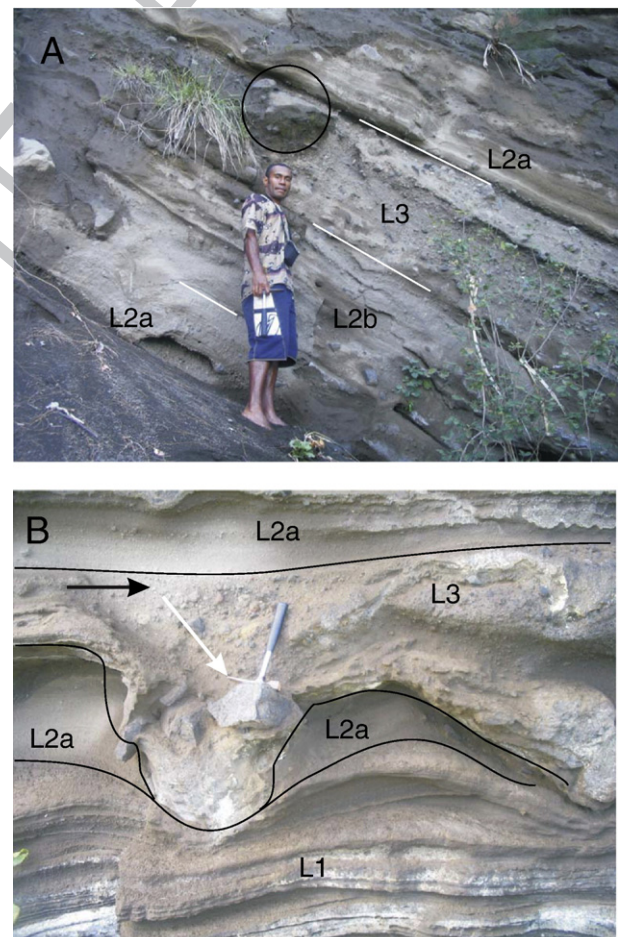


**Fig. 8.** Steeply dipping phreatomagmatic succession in proximal areas of the NE coastline half section of the phreatomagmatic volcano (A). Note the large volcanic lithic block in L3 with no impact sag under. On “B” a volcanic lithic block caused deep impact crater (white arrow marks transportation direction) that captured other coarser grained fragments from the passing pyroclastic density currents (black arrow marks the transportation direction).



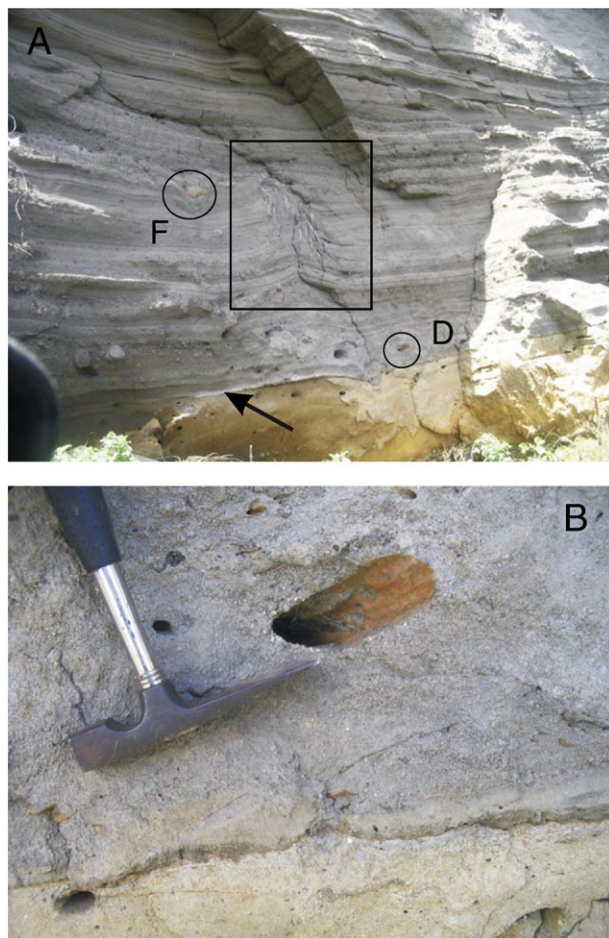


**Fig. 9.** Base of a pyroclastic density current succession (A) accumulated over an immature soil horizon (contact is shown by a black arrow). The pyroclastic density current deposits contain few fragments (F) from older phreatomagmatic lapilli tuffs as well as debris (D) of broken tree branches. Standing tree remnants marked by a rectangle. On "B" a close up view shows a bed flattened vegetation remnant.

unit is similar to those described from other phreatomagmatic volcanic fields such as Auckland, New Zealand (Marra et al., 2006). The thin tree trunks and disrupted branches show no signs of thermal alteration about one km away from the vent. This indicates that the passing pyroclastic density currents had low velocity and low temperatures (Gurioli et al., 2002). The plastering effects on standing tree trunks and bedding-parallel branches indicate that cohesive, moisture-rich pyroclastic density currents passed through the vegetation cover.

The contact between the middle and top pyroclastic units is obscure, but textural differences of the pyroclastic units, differing paleocurrent indicators and the overall 3D architecture imply that the topmost section of the exposures are sourced from the south from the 4B vent site (on Fig. 1C). The majority of the lower and coastal exposures are deposits sourced from the eastern 4C phreatomagmatic volcano.

Distal pyroclastic successions associated with small-volume monogenetic volcanoes such as scoria cones and phreatomagmatic volcanoes in NE Ambae crop out near the coastline of Saratamata village (Fig. 10). These sections are important from an archaeological point of view because human occupation sites have been identified between individual packages of pyroclastic units, a few dm-to-m thick, derived from scoria cone and phreatomagmatic volcano (Bedford et al., 1999; Bedford, 2006; Cronin et al., 2008). This indicates that phreatomagmatic volcanoes and other rift-edge scoria cones were active during the known human occupation times of Ambae, which is estimated to be about 3000 years before present and new data indi-

cates eruptive activity as young as <500 and <300 yr B.P. (Bedford, 2006; Cronin et al., 2008).

Near the Saratamata coast (toward Airport turnoff/Navonda) a section exposes 4 well-defined volcanic units (Figs. 1 and 10). The succession is topped by an about 10 cm thick, dark brown, nutty structured silt loam with common scoria fine lapilli and moderately rounded cobbles and pebbles of volcanic lithic and coral fragments (Unit 4). In these topmost beds, brown unadorned pottery fragments (up to 5 cm diameter) have been recovered. These beds are interpreted to be locally reworked volcanic ash and lapilli.

This unit has a gradational contact with a package of primary and secondary volcaniclastic beds (Unit 3). The topmost part of this unit is a 2–10 cm thick and 30–50 cm long patches of deep brown fine scoria lapilli inferred to be primary air-fall lapilli, derived from a nearby scoria cone. This primary succession has a gradational contact downward to a 20–30 cm thick, brown, nutty structured silt loam with rare scoria lapilli and rare rounded and angular volcanic rock pebbles. This succession is inferred to be locally reworked volcanic ash and lapilli. In this bed, rare unadorned pottery fragments (up to 4 cm diameter) have been identified. Below this bed with a gradational contact a 20–30 cm thick, structureless, yellow brown silt loam with rare grey and red scoria coarse lapilli fragments and rare charcoal fragments have been identified. This bed has been interpreted to be also locally reworked volcanic ash and lapilli.

Below Unit 3, a succession of Unit 2 with a sharp contact can be traced. It is topped by a 15 cm thick, greyish brown, bedded fine-medium ash tuff. It is bedded on a mm-cm scale, including vesiculated beds and accretionary lapilli-bearing beds and mantling underlying topography. On the basis of these features, these deposits are interpreted to be dominantly volcanic fall units, but include distal pyroclastic surge deposits derived from a nearby phreatomagmatic volcano. With a sharp contact, 5–10 cm thick, black/dark grey fine scoria lapilli unit crops out and are interpreted to be primary volcanic airfall deposits, derived from a nearby scoria cone, probably genetically related to the unit above. This unit sits with a sharp contact on a 40 cm thick, greyish brown to pale yellow brown silt loam with yellow brown weathered fine scoria lapilli and red angular coarse lapilli. Grey, angular and subrounded dense lava fragments, coral fragments and reddish coarse scoria pebbles are concentrated in patches along the upper 5–10 cm of the unit; pottery fragments, up to 5 cm in diameter, are also rarely present along this horizon. This unit is interpreted to be locally reworked ash and lapilli.

The base of this succession (Unit 1) develops with sharp contact. It is at least 50 cm thick, greyish brown, finely bedded, medium-to-fine ash tuff. Bedding can be traced on a mm-to-cm scale with common accretionary lapilli horizons. Mantle bedding is apparent and indicates predominantly fall origin. This unit also includes distal pyroclastic surge deposits derived from a nearby phreatomagmatic volcano.

A very similar succession has been identified closer to Saratamata Village. In this distal succession, rare pottery fragments are also identified between primary volcanic units, indicating human occupation and recurrence of small-volume monogenetic volcanism both with magmatic and phreatomagmatic explosive activity in the NE rift edge of Ambae.

The presence of cultural horizons between distal pyroclastic units associated with small-volume explosive eruptions from local sources such as scoria cones and phreatomagmatic volcanoes indicates that volcanism in this part of the island is young (certainly younger than 3000 years B.P.). The cultural horizons interbedded with locally reworked distal pyroclastic units also indicate that there were relatively long (decades to hundreds of years) breaks in eruptive activity, long enough to develop human settlements over volcanic eruption-modified landscapes. At present, the recurrence rate and the timing of individual volcanic events couldn't be established because of the lack of reliable age data and possibility of lateral correlation of individual pyroclastic units (due to tropical vegetation cover). However, the

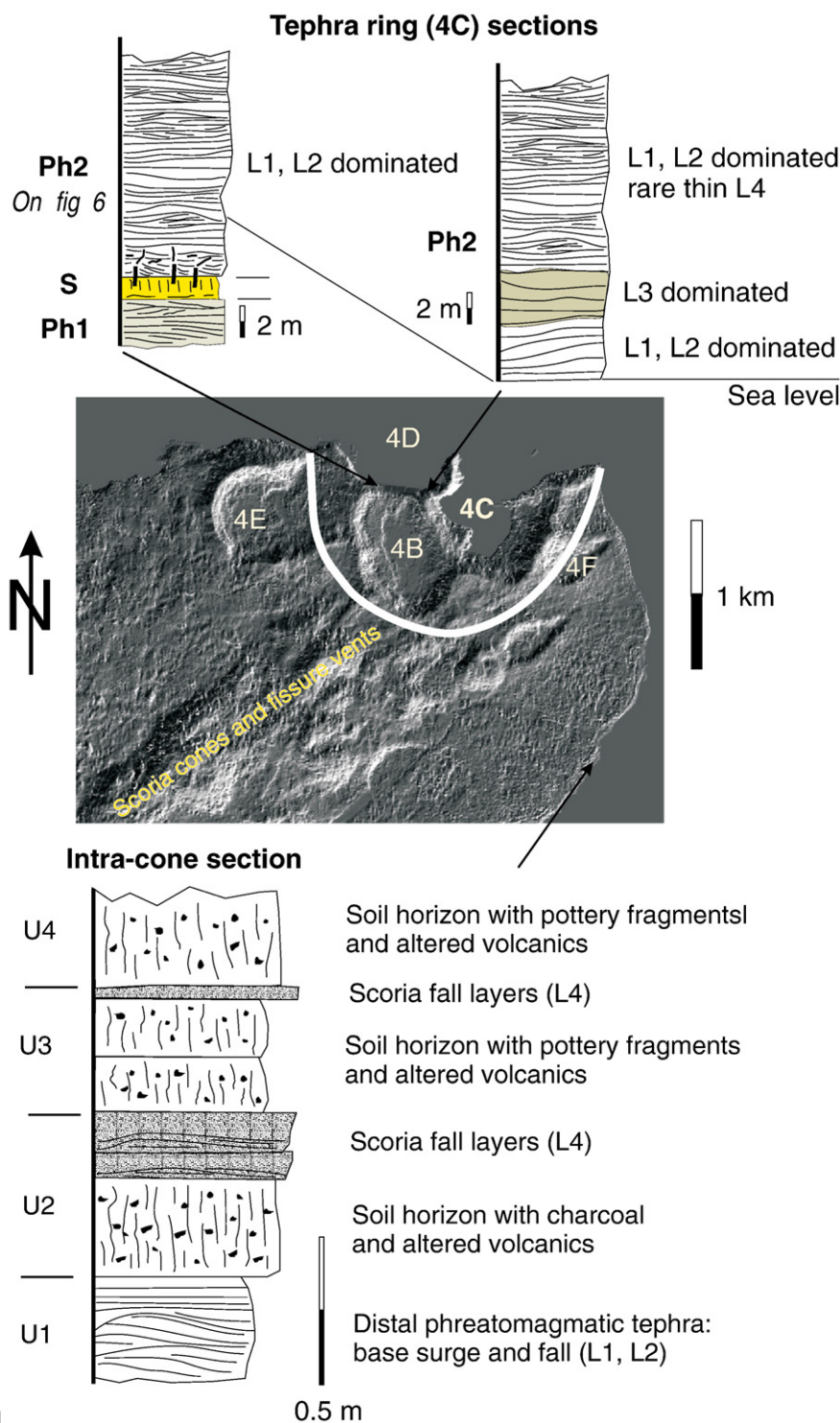


**Fig. 10.** Simplified stratigraphy logs from the cone building pyroclastic succession of one of the major phreatomagmatic volcano and from intra-cone fields in the coastal plains of eastern Ambae. Lithofacies codes are identical to those described in the text.

489 explosive volcanism was certainly young and repeated in this region of  
 490 the island, and it has affected almost the entire NE edge of the island in  
 491 each eruptive phase.

## 492 10. Discussion

493 At least three major eruptive events can be distinguished in this  
 494 restricted location, showing that the locus of volcanic eruptions has  
 495 remained stable at the NE edge of Ambae. Occurrence of soils between

the eruptive units implies that renewed periodic phreatomagmatic 496  
 volcanism is a feature of this location. The well distinguished units 497  
 from sporadic distal exposures confirm the repetition of volcanic 498  
 events and their effect on landscape evolution of NE Ambae. This 499  
 implies that the rift edge(es) on Ambae should be viewed as high 500  
 volcanic hazard risk areas (Fig. 1). During the course of the eruption in 501  
 December 2005, about half of the total population of the island was 502  
 displaced in the area of phreatomagmatic volcanoes in the NE rift edge 503  
 considering that area safe. 504

The stratigraphic and archeological features of the preserved pyroclastic successions from both proximal and distal sections give evidence of repeated phreatomagmatic activity and attendant scoria cone-building eruptions in NE Ambae during the recent times, at least since human occupation took place in this part of the island. Textural features from the proximal half sections of the phreatomagmatic volcanoes such as the presence of accretionary lapilli throughout the sections indicate that the pyroclastic density currents were wet, comprising condensed water, but they were not wet enough to generate water-saturated tephra beds and associated deformation (Sohn and Chough, 1989; Rosi, 1992; Schumacher and Schmincke, 1995). This indicates that the phreatomagmatic explosions involved close-to-optimal magma:water ratios to cause powerful explosions, and no surplus water was in the system during the magma and water interaction (Wohletz and Sheridan, 1983). The relatively high proportion of the accidental lithic fragments throughout the pyroclastic deposits suggests that excavation of country rocks was continual and/or the volcanic conduits were partially collapsed on occasions during the eruptions. The coarse-grained tuff-breccia horizons of the L3 lithofacies also indicate vent-clearing events, and/or major conduit wall collapse in the course of the eruptions. They were probably emplaced by direct pyroclast jets. The mid-level pyroclastic unit lies on a formerly vegetated surface, indicating a subaerial depositional environment. The presence of country rock in the phreatomagmatic pyroclastic succession suggests that the eruption of the 4C phreatomagmatic volcano took place in a near sea-level coastal plain. Local legends and traditional stories mention that a fresh water lake was in the volcanic depression before the outer crater wall was breached by the sea (Cronin et al., 2004).

The depositional features and the areal distribution pattern of the preserved pyroclastic units suggest that the entire NE edge of the island would be affected predominantly by pyroclastic density currents, scoria fall events and direct pyroclast jets from phreatomagmatic volcanoes in a future eruption, assuming similar eruptive activity to those that formed the preserved tuff rings. The eruption duration of a single phreatomagmatic volcano is estimated to be in the range of days to weeks on the bases of recent analogies from worldwide examples (Thorarinsson, 1967; Kokelaar, 1983; Cole et al., 2001; Németh et al., 2006). Distal tephra would most certainly affect most of the NE peninsula of Ambae given a future eruption of similar nature in this part of the island. A new phreatomagmatic eruption site would constructed a circular crater 500–1000 m wide, with distal tephra capable of reaching a few kilometres away. It is generally assumed that a new vent would not open in the same place as any previous vent, although recurrence of eruptions in the same site with slightly shifted vents are known from several volcanic fields (Houghton and Schmincke, 1989; Németh et al., 2001; Németh and White, 2003; Auer et al., 2007; Brand and White, 2007). The stratigraphic relationships of the proximal and distal pyroclastic units of the phreatomagmatic volcanoes in NE Ambae suggest formation vent sites can be very closely located and does not rule out them being overlapping. This is also likely because vent sites are highly restricted to the central part of the rift zone, controlled by magma feeding along lateral dykes. A good example for this is known from the rift edge volcanic fields of the nearby Ambrym Island. In Ambrym Island, in 1913, new phreatomagmatic eruptions occurred in the broad crater of an older phreatomagmatic tuff ring (Frater, 1917; Gregory, 1917). This fact implies that there can be immediate volcanic hazards for Ambae where recent human development (schools, water reservoirs, agricultural activity) favours the relatively flat and open spaces provided by crater floors in NE Ambae.

In the case of the neighbouring Ambrym Island, there are clear eyewitness accounts as well as geological data demonstrating a coupling mechanism between summit eruptions and rift-edge, dominantly phreatomagmatic, explosive activity. In Ambrym, rift-edge volcanism is almost exclusively predated by volcano-seismic and

eruptive activity in the summit region of the island. Initial summit eruptions were followed by rift-edge volcanism just days after as it has been demonstrated in 1894 (Purey-Cust, 1896) and 1913 (Frater, 1917; Gregory, 1917). This coupling mechanism was the reason to avoid tragic loss of life in 1913 when the new tuff ring formed in the older tuff ring region occupied by a missionary hospital (Frater, 1917; Gregory, 1917). Similar coupling mechanisms between summit and rift-edge volcanism are also anticipated at Ambae, although no oral traditions or historic evidence is known to support this (Cronin et al., 2004).

Ambae rift-edge volcanism is very similar to that at many other volcanoes of similar structure, including Taveuni in Fiji, where dozens of monogenetic volcanoes developed on a basal lava shield along the well-defined rift (Cronin and Neall, 2001). Eruptions along the rift axis and edges show no characteristic time and space evolution trend apart from occurring with highest frequency in central parts of the rift where greater thicknesses of volcanic units overlap to build the highest ground (Cronin et al., 2001). In spite of the apparent similarity of random distribution of eruptive events along the rift, Taveuni lacks a well-defined central volcanic edifice such as at Ambae and Ambrym. Similar comparisons could be drawn between Ambae and the main islands of Western Samoa (Upolu and Savai'i). In Upolu and Savai'i rift-edge phreatomagmatism is well known (Keating, 1991; Cronin et al., 2000; Cronin et al., 2006), although their time relationship with other rift axis volcanism is unknown and inferred to be random (Kear and Wood, 1959), similar to the case of Ambae. The Western Samoan islands are similar to Taveuni with no well-defined central volcano other than lava shields.

Development of rift-edge volcanoes and volcanic fields with extensive phreatomagmatism seems to show a gradual transition from single composite volcanoes (common volcanic islands) to more well-defined rift-edge volcanic fields. This transition is well defined by initial rift-axis cone formation in the flank of Lopevi in Vanuatu (Warden, 1967; Cronin et al., 2003). Such initial rift-axis volcanism commonly forms phreatomagmatic volcanoes near the coastlines. It is also known from volcanic islands that localisation of well-defined rift axis may take time in the evolution of the volcano, and in its initial stage small-volume volcanoes may form apparently randomly around the central vent complex, many of them with phreatomagmatic eruption history close to the sea level such as the case in Izu-Oshima (Ida, 1995; Sumner, 1998) and Miyakejima (Geshi et al., 2002; Yamaoka et al., 2005) in Japan.

## 11. Conclusion

Rift-edge phreatomagmatism has played an important role in the volcanic evolution of Ambae, and it generated potentially dangerous, destructive eruptions. The NE rift-edge of Ambae Island is a complex monogenetic volcanic field with numerous scoria cones and at least five large (km-wide) tuff rings/cones. The local legends, traditional stories and, most importantly, artefacts from human occupation embedded within scoria fall and phreatomagmatic tephra deposits indicate young absolute ages (<3000 yr B.P.) and repeated eruptions in this part of Ambae Island. The lack of eyewitness accounts as well as references from oral traditions from village communities is unable to provide clear evidence of possible connections between central, summit-vent eruptions and the formation of the rift-edge volcanic fields. However, by comparison to neighbouring volcanoes of similar structure (Ambrym and Lopevi) suggests a close coupling with central volcanism is very likely. The pyroclastic density current-dominated pyroclastic successions from exposed in the tuff cones/rings suggest significant destructive forces from this volcanism, which has the potential to affect the entirety of the northern area with tephra fall and surges. Rift edges and broad flat crater floors in these areas on Ambae and other similar volcanoes are popular sites for infrastructure development. However, this practice may lead to exacerbating

635 community vulnerability to re-awakening phreatomagmatism in  
636 these areas.

### 637 Acknowledgements

638 The authors acknowledge support from FRST Post-Doctoral fellow-  
639 ship MAUX0405 (KN), and FRST-PCGST contract MAUX0401 (SJC). We  
640 are grateful to the traditional landowners in this area for hospitality,  
641 advice and access to all field sites. Journal reviewers' suggestions  
642 significantly improved the quality of this paper.

### 643 References

644 Arana, V., Felpeto, A., Astiz, M., Garcia, A., Ortiz, R., Abella, R., 2000. Zonation of the main  
645 volcanic hazards (lava flows and ash fall) in Tenerife, Canary Islands. A proposal for  
646 a surveillance network. *J. Volcanol. Geotherm. Res.* 103, 377–391.  
647 Aranda-Gomez, J.J., Luhr, J.F., 1996. Origin of the Joya Honda maar, San Luis Potosi,  
648 Mexico. *J. Volcanol. Geotherm. Res.* 74, 1–18.  
649 Auer, A., Martin, U., Németh, K., 2007. The Fekete-hegy (Balaton Highland Hungary)  
650 "soft-substrate" and "hard-substrate" maar volcanoes in an aligned volcanic  
651 complex – implications for vent geometry, subsurface stratigraphy and the  
652 palaeoenvironmental setting. *J. Volcanol. Geotherm. Res.* 159, 225–245.  
653 Bedford, S., 2006. Pieces of the Vanuatu Puzzle: archaeology of the north, south and  
654 centre, Terra Australis. Pandanus Books, Research School of Pacific and Asian  
655 Studies, Australian National University, Canberra. 326 pp.  
656 Bedford, S., Spriggs, M., Regenvanu, R., 1999. The Australian National University-  
657 Vanuatu Cultural Centre Archaeology Project, 1994–97: Aims and results. *Oceania*  
658 70, 16–24.  
659 Blot, C., Priam, R., 1962. Volcanisme ed séismicité dans l'archipel des Nouvelles-  
660 Hébrides. ORSTOM, Nouméa. 20 pp.  
661 Bogaard, P.v.d., Schmincke, H.-U., 1984. The eruptive center of the Late Quaternary  
662 Laacher See Tephra. *Geol. Rundsch.* 73, 933–980.  
663 Boubekraoui, S., Courteaud, M., Aubert, M., Albouy, Y., Coudray, J., 1998. New insights  
664 into the hydrogeology of a basaltic shield volcano from a comparison between self-  
665 potential and electromagnetic data: Piton de la Fournaise, Indian Ocean. *J. Appl.*  
666 *Geophys.* 40, 165–177.  
667 Brand, B.D., White, C.M., 2007. Origin and stratigraphy of phreatomagmatic deposits at  
668 the Pleistocene Sinker Butte Volcano, Western Snake River Plain, Idaho. *J. Volcanol.*  
669 *Geotherm. Res.* 160, 319–339.  
670 Büchel, G., Lorenz, V., 1993. Syn- and post-eruptive mechanism of the Alaskan Ukinrek  
671 maars in 1977. In: Negendank, J.F.W., Zolitschka, B. (Eds.), *Paleolimnology of*  
672 *European Maar Lakes*. Springer-Verlag, Berlin, Heidelberg, pp. 15–60.  
673 Calmant, S., Pelletier, B., Lebellegard, P., Bevis, M., Taylor, F.W., Phillips, D.A., 2003. New  
674 insights on the tectonics along the New Hebrides subduction zone based on GPS  
675 results. *J. Geophys. Res.* 108 (B6).  
676 Carn, S.A., Watts, R.B., Thompson, G., Norton, G.E., 2004. Anatomy of a lava dome collapse:  
677 the 20 March 2000 event at Soufriere Hills Volcano, Montserrat. *J. Volcanol. Geotherm.*  
678 *Res.* 131, 241–264.  
679 Carracedo, J.C., Day, S.J., Guillou, H., Gravelstock, P., 1999. Later stages of volcanic  
680 evolution of La Palma, Canary Islands: rift evolution, giant landslides, and the  
681 genesis of the Caldera de Taburiente. *Geol. Soc. Am. Bull.* 111, 755–768.  
682 Chough, S.K., Sohn, Y.K., 1990. Depositional mechanics and sequences of base surges,  
683 Songaksan tuff ring, Cheju Island, Korea. *Sedimentology* 37, 1115–1135.  
684 Cole, P.D., Guest, J.E., Queiroz, G., Wallenstein, N., Pacheco, J.M., Gaspar, J.L., Ferreira, T.,  
685 Duncan, A.M., 1999. Styles of volcanism and volcanic hazards on Furnas volcano, Sao  
686 Miguel, Azores. *J. Volcanol. Geotherm. Res.* 92, 39–53.  
687 Cole, P.D., Guest, J.E., Duncan, A.M., Pacheco, J.M., 2001. Capelinhos 1957–1958, Faial,  
688 Azores: deposits formed by an emergent surtseyan eruption. *Bull. Volcanol.* 63,  
689 204–220.  
690 Cronin, S.J., Neall, V.E., 2001. Holocene volcanic geology, volcanic hazard, and risk on  
691 Taveuni, Fiji. *N. Z. J. Geol. Geophys.* 44, 417–437.  
692 Cronin, S.J., Taylor, P.W., Malef, F., 2000. Final report – Savai'i, volcanic hazards project  
693 Samoa, October 2000. SOPAC Technical Report (Suva, Fiji) 343, 1–34.  
694 Cronin, S.J., Bebbington, M., Lai, C.D., 2001. A probabilistic assessment of eruption  
695 recurrence on Taveuni volcano, Fiji. *Bull. Volcanol.* 63, 274–288.  
696 Cronin, S.J., Platz, T., Charley, D., Turner, M., 2003. The June 2003 eruption of Lopevi  
697 Volcano, Vanuatu. *Geol. Soc. New Zealand Misc. Publ.*, vol. 116A, p. 42.  
698 Cronin, S.J., Gaylord, D.R., Charley, D., Alloway, B.V., Wallez, S., Esau, J.W., 2004. Participatory  
699 methods of incorporating scientific with traditional knowledge for volcanic hazard  
700 management on Ambae Island, Vanuatu. *Bull. Volcanol.* 66, 652–668.  
701 Cronin, S.J., Bonte-Grapentin, M., Németh, K., 2006. Samoa technical report – review of  
702 volcanic hazard maps for Savai'i and Upolu. EU-SOPAC Project Report 59, 1–27.  
703 Cronin, S.J., Németh, K., Neall, V.E., 2008. Volcanism and Archaeology. In: Pearsall, D.M.  
704 (Ed.), *Encyclopedia of Archaeology*. Academic Press, New York, pp. 2185–2196.  
705 Crowe, B.M., Fisher, R.V., 1973. Sedimentary structures in base-surge deposits with  
706 special reference to cross-bedding, Ubehebe Craters, Death Valley, California. *Geol.*  
707 *Soc. Am. Bull.* 84, 663–682.  
708 Day, S.J., da Silva, S., Fonseca, J., 1999. A past giant lateral collapse and present-day flank  
709 instability of Fogo, Cape Verde Islands. *J. Volcanol. Geotherm. Res.* 94, 191–218.  
710 de la Rüe, A.E., 1956. La géologie des Nouvelles-Hébrides. *J. Soc. Océanistes* 12, 63–98.  
711 Dellino, P., Frazzetta, G., La Volpe, L., 1990. Wet surge deposits at La Fossa di Vulcano:  
712 depositional and eruptive mechanisms. *J. Volcanol. Geotherm. Res.* 43, 215–233.

Dellino, P., Isaia, R., La Volpe, L., Orsi, G., 2004a. Interaction between particles  
713 transported by fallout and surge in the deposits of the Agnano-Monte Spina  
714 eruption (Campi Flegrei, Southern Italy). *J. Volcanol. Geotherm. Res.* 133, 193–210.  
715 Dellino, P., Isaia, R., Veneruso, M., 2004b. Turbulent boundary layer shear flows as a  
716 approximation of base surges at Campi Flegrei (Southern Italy). *J. Volcanol.*  
717 *Geotherm. Res.* 133, 211–228.  
718 Dellino, P., La Volpe, L., 2000. Structures and grain size distribution in surge deposits as a  
719 tool for modelling the dynamics of dilute pyroclastic density currents at La Fossa di  
720 Vulcano (Aeolian Islands, Italy). *J. Volcanol. Geotherm. Res.* 96, 57–78.  
721 Fisher, R.V., 1977. Erosion by volcanic base-surge density currents: U-shaped channels.  
722 *Geol. Soc. Am. Bull.* 88, 1287–1297.  
723 Fisher, R.V., Waters, A.C., 1970. Base surge bed forms in maar volcanoes. *Am. J. Sci.* 268,  
724 157–180.  
725 Frater, M., 1917. Volcanic eruption, Ambrym Island (1913). *Geol. Mag.* 6, 496–503.  
726 Garaebiti, E., 2000. Analyse morphologique des Risques Volcaniques d'Aoba (Vanuatu).  
727 Travail d'Etude et de Recherche Maitrise 1999–2000. Département de Sciences de la  
728 Terre, pp. 1–30.  
729 Geshi, N., Shimano, T., Chiba, T., Nakada, S., 2002. Caldera collapse during the 2000  
730 eruption of Miyakejima Volcano, Japan. *Bull. Volc.* 64, 55–68.  
731 Gladstone, C., Sparks, R.S.J., 2002. The significance of grain size breaks in turbidites and  
732 pyroclastic density current deposits. *J. Sedim. Res.* 72, 182–191.  
733 Godchaux, M.M., Bonnichsen, B., Jenks, M.D., 1992. Types of phreatomagmatic volcanoes  
734 in the Western Snake River Plain, Idaho, USA. *J. Volcanol. Geotherm. Res.* 52, 1–25.  
735 Gregory, J.W., 1917. The Ambrym eruptions of 1913–1914. *Geol. Mag.* December 1917,  
736 496–503.  
737 Gurioli, L., Cioni, R., Sbrana, A., Zanella, E., 2002. Transport and deposition of pyroclastic  
738 density currents over an inhabited area: the deposits of the AD 79 eruption of  
739 Vesuvius at Herculaneum, Italy. *Sedimentology* 49, 929–953.  
740 Gutmann, J.T., 2002. Strombolian and effusive activity as precursors to phreatomag-  
741 matism: eruptive sequence at maars of the Pinacate volcanic field, Sonora, Mexico.  
742 *J. Volcanol. Geotherm. Res.* 113, 345–356.  
743 Houghton, B.F., Schmincke, H.U., 1989. Rothenberg scoria cone, East Eifel; a complex  
744 strombolian and phreatomagmatic volcano. *Bull. Volcanol.* 52, 28–48.  
745 Ida, Y., 1995. Magma chamber and eruptive processes at Izu-Oshima Volcano, Japan –  
746 buoyancy control of magma migration. *J. Volcanol. Geotherm. Res.* 66, 53–67.  
747 Join, J.L., Folio, J.L., Robineau, B., 2005. Aquifers and groundwater within active shield  
748 volcanoes. Evolution of conceptual models in the Piton de la Fournaise volcano.  
749 *J. Volcanol. Geotherm. Res.* 147, 187–201.  
750 Kear, D., Wood, B.L., 1959. The geology and hydrology of Western Samoa. *New Zealand*  
751 *Geol. Surv. Bull.* 63, 1–90.  
752 Keating, B.H., 1991. Geology of the Samoan Islands. In: Keating Barbara, H., Bolton Barrie,  
753 R. (Eds.), *Geology and offshore mineral resources of the Central Pacific Basin*.  
754 Circum-Pacific Council for Energy and Mineral Resources, Earth Science rics.  
755 Circum-Pacific Council for Energy and Mineral Resources, Houston, TX, United ates,  
756 pp. 127–178.  
757 Kokelaar, B.P., 1983. The mechanism of Surtseyan volcanism. *J. Geol. Soc. London* 140,  
758 939–944.  
759 Kokelaar, P., 1986. Magma-water interactions in subaqueous and emergent basaltic  
760 volcanism. *Bull. Volcanol.* 48, 275–289.  
761 Lajoie, J., Lanzafame, G., Rossi, P.L., Tranne, C.A., 1992. Lateral facies variations in  
762 hydromagmatic pyroclastic deposits at Linosa, Italy. *J. Volcanol. Geotherm. Res.* 54,  
763 135–143.  
764 Lardy, M., Maltera, M., Charley, D., 1997. Mission on LOMBENBEN Volcano (Ambae  
765 Island) November 25 to 27, 1996 and bathymetric Measurements at Voui Lake.  
766 Notes Techniques, Science de la Terre, Géologie-Geophysique, représentation de  
767 l'ORSTOM en république de Vanuatu, p. 3.  
768 Leat, P.T., Thompson, R.N., 1988. Miocene hydrovolcanism in NW Colorado, USA,  
769 fuelled by explosive mixing of basic magma and wet unconsolidated sediment. *Bull.*  
770 *Volcanol.* 50, 229–243.  
771 Lorenz, V., 1974a. Studies of the Surtsey tephra deposits. Surtsey Research Program  
772 Report 7, 72–79.  
773 Lorenz, V., 1974b. Vesiculated tuffs and associated features. *Sedimentology* 21, 273–291.  
774 Lorenz, V., 1986. On the growth of maars and diatremes and its relevance to the  
775 formation of tuff rings. *Bull. Volcanol.* 48, 265–274.  
776 Lorenz, V., 2007. Syn- and post-eruptive hazards of maar-diatreme volcanoes. *J. Volcanol.*  
777 *Geotherm. Res.* 159, 285–312.  
778 Lorenz, V., Kurszlaukis, S., 2007. Root zone processes in the phreatomagmatic pipe  
779 emplacement model and consequences for the evolution of maar-diatreme  
780 volcanoes. *J. Volcanol. Geotherm. Res.* 159, 4–32.  
781 Malheiro, A., 2006. Geological hazards in the Azores archipelago: volcanic terrain  
782 instability and human vulnerability. *J. Volcanol. Geotherm. Res.* 156, 158–171.  
783 Marra, M.J., Alloway, B.V., Newnham, R.M., 2006. Paleoenvironmental reconstruction of  
784 a well-preserved Stage 7 forest sequence catastrophically buried by basaltic  
785 eruptive deposits, northern New Zealand. *Quar. Sci. Rev.* 25, 2143–2161.  
786 Martin, U., Németh, K., 2005. Eruptive and depositional history of a Pliocene tuff ring  
787 that developed in a fluvio-lacustrine basin: Kissonlyó volcano (western Hungary).  
788 *J. Volcanol. Geotherm. Res.* 147, 342–356.  
789 Martin, U., Németh, K., 2006. How Strombolian is a "Strombolian" scoria cone? Some  
790 irregularities in scoria cone architecture from the Transmexican Volcanic Belt, near  
791 Volcan Ceboruco, (Mexico) and Al Haruj (Libya). *J. Volcanol. Geotherm. Res.* 155,  
792 104–118.  
793 Mastrolorenzo, G., 1994. Averno tuff ring in Campi-Flegrei (South Italy). *Bull. Volcanol.*  
794 56, 561–572.  
795 Mattioli, G.S., Jansma, P.E., Jaramillo, L., Smith, A.L., 1996. A desktop image processing  
796 and photogrammetric method for rapid volcanic hazard mapping: Application to  
797 air-photo interpretation of Mount Pelee, Martinique. *Bull. Volcanol.* 58, 401–410.  
798

- 799 Meffre, S., Crawford, A.J., 2001. Collision tectonics in the New Hebrides arc (Vanuatu).  
800 Island Arc 10, 33–50.
- 801 Moore, J.G., 1967. Base surge in recent volcanic eruptions. Bull. Volcanol. 30, 337–363.
- 802 Mueller, W.U., Garde, A.A., Stendal, H., 2000. Shallow-water, eruption-fed, mafic  
803 pyroclastic deposits along a Paleoproterozoic coastline: Kangerluluk volcano-  
804 sedimentary sequence, southeast Greenland. Precambrian Res. 101, 163–192.
- 805 Munn, S., Walter, T.R., Klugel, A., 2006. Gravitational spreading controls rift zones and  
806 flank instability on El Hierro, Canary Islands. Geol. Mag. 143, 257–268.
- 807 Németh, K., White, J.D.L., 2003. Reconstructing eruption processes of a Miocene  
808 monogenetic volcanic field from vent remnants: Waipiata Volcanic Field, South  
809 Island, New Zealand. J. Volcanol. Geotherm. Res. 124, 1–21.
- 810 Németh, K., Cronin, S., 2007. Syn- and post-eruptive erosion, gully formation, and  
811 morphological evolution of a tephra ring in tropical climate erupted in 1913 in West  
812 Ambrym, Vanuatu. Geomorphology 86, 115–130.
- 813 Németh, K., Martin, U., Harangi, S., 2001. Miocene phreatomagmatic volcanism at  
814 Tihany (Pannonian Basin, Hungary). J. Volcanol. Geotherm. Res. 111, 111–135.
- 815 Németh, K., Cronin, S.J., Charley, D., Harrison, M., Garae, E., 2006. Exploding lakes in  
816 Vanuatu – “Surtseyan-style” eruptions witnessed on Ambae Island. Episodes 29,  
817 87–92.
- 818 Ort, M.H., Dallegre, T.A., Vazquez, J.A., White, J.D.L., 1998. Volcanism and sedimentation  
819 in the Mio-Pliocene Bidahochi Formation, Navajo Nation, NE AZ. In: Duebendorfer,  
820 E. (Ed.), Geologic Excursions in northern and Central Arizona. Field trip Guidebook  
821 for Geological Society of America Rocky Mountain Section Meeting, Arizona.  
822 Geological Society of America, Flagstaff, Arizona, pp. 35–57.
- 823 Purey-Cust, H.E., 1896. The eruption of Ambrym Volcano, New Hebrides, South-West  
824 Pacific, 1894. Geograph. J. VIII, 585–602.
- 825 Robin, C., Eissen, J.P., Monzier, M., 1993. Giant tuff cone and 12-km-wide associated  
826 caldera at Ambrym Volcano (Vanuatu, New-Hebrides-Arc). J. Volcanol. Geotherm.  
827 Res. 55, 225–238.
- 828 Robin, C., Monzier, M., Lardy, M., Regnier, M., Metaxian, J.-P., Decourt, R., Charley, D.,  
829 Ruiz, M., Eissen, J.-P., 1995. Increased steam emissions and seismicity in early  
830 March; evacuation preparations made, Aoba, Vanuatu. Bull. Glob. Volcanism Netw.  
831 20, 2.
- 832 Rosi, M., 1992. A model for the formation of vesiculated tuff by the coalescence of  
833 accretionary lapilli. Bull. Volcanol. 54, 429–434.
- 834 Schmincke, H.-U., Fisher, R.V., Waters, A., 1973. Antidune and chute and pool structures  
835 in the base surge deposits of the Laacher See area, Germany. Sedimentology 20,  
836 553–574.
- 837 Schumacher, R., Schmincke, H.-U., 1995. Models for the origin of accretionary lapilli.  
838 Bull. Volcanol. 56, 626–639.
- 839 Schumacher, R., Schmincke, H.U., 1991. Internal structure and occurrence of accre-  
840 tionary lapilli – a case study at Laacher See volcano. Bull. Volcanol. 53, 612–634.
- 841 Scolamacchia, T., Macias, J.L., 2005. Distribution and stratigraphy of deposits produced  
842 by diluted pyroclastic density currents of the 1982 eruption of El Chichon volcano,  
843 Chiapas, Mexico. Rev. Mexicana Cienc. Geol. 22, 159–180.
- 844 Sohn, Y.K., 1996. Hydrovolcanic processes forming basaltic tuff rings and cones on Cheju  
845 Island, Korea. Geol. Soc. Am. Bull. 108, 1199–1211.
- Sohn, Y.K., Chough, S.K., 1989. Depositional processes of the Suwolbong Tuff Ring, Cheju  
846 Island (Korea). Sedimentology 36, 837–855. 847
- Sohn, Y.K., Chough, S.K., 1992. The Ilchulbong tuff cone, Cheju Island, South-Korea –  
848 depositional processes and evolution of an emergent, Surtseyan-type tuff cone. 849  
Sedimentology 39, 523–544. 850
- Sulpizio, R., Mele, D., Dellino, P., La Volpe, L., 2007. Deposits and physical properties of  
851 pyroclastic density currents during complex Subplinian eruptions: the AD 472  
852 (Pollena) eruption of Somma-Vesuvius, Italy. Sedimentology 54, 607–635. 853
- Sumner, J.M., 1998. Formation of clastogenic lava flows during fissure eruption and  
854 scoria cone collapse: the 1986 eruption of Izu-Oshima Volcano, eastern Japan. Bull.  
855 Volcanol. 60, 195–212. 856
- Thorarinsson, S., 1967. Surtsey. The New Island in the North Atlantic. The Viking Press,  
857 New York. 47 pp. 858
- Vazquez, J.A., Ort, M.H., 2006. Facies variation of eruption units produced by the passage  
859 of single pyroclastic surge currents, Hopi Buttes volcanic field, USA. J. Volcanol.  
860 Geotherm. Res. 154, 222–236. 861
- Violette, S., de Marsily, G., Carbonnel, J.P., Goblet, P., Ledoux, E., Tijani, S.M., Vouille, G.,  
862 2001. Can rainfall trigger volcanic eruptions? A mechanical stress model of an active  
863 volcano: 'Piton de la Fournaise'. Reunion Island, vol. 13. Terra Nova, pp. 18–24. 864
- Walter, T.R., Troll, V.R., Cailleau, B., Belousov, A., Schmincke, H.U., Amelung, F., von der  
865 Bogaard, P., 2005. Rift zone reorganization through flank instability in ocean island  
866 volcanoes: an example from Tenerife, Canary Islands. Bull. Volcanol. 67, 281–291. 867
- Warden, A.J., 1967. The geology of the Central Islands. New Hebrides Geol. Surv. Reports,  
868 Port Vila. 108 pp. 869
- Warden, A.J., 1970. Evolution of Aoba caldera volcano, New Hebrides. Bull. Volcanol. 34,  
870 107–140. 871
- Waters, A.C., Fisher, R.V., 1971. Base surges and its deposits: Capelinhos and Taal  
872 volcanoes. J. Geophys. Res. 76, 5596–5614. 873
- White, J.D.L., 1989. Basic elements of maar-crater deposits in the Hopi Buttes volcanic  
874 field, Northeastern Arizona, USA. J. Geol. 97, 117–125. 875
- White, J.D.L., Schmincke, H.U., 1999. Phreatomagmatic eruptive and depositional  
876 processes during the 1949 eruption on La Palma (Canary Islands). J. Volcanol.  
877 Geotherm. Res. 94, 283–304. 878
- Williams, C.E.F., Warden, A.J., 1964. Progress report of the Geological Survey for 1959–  
879 62. New Hebrides Geol. Surv. Rep. Port Vila, p. 75. 880
- Wohletz, K.H., Sheridan, M.F., 1979. A model of pyroclastic surge. Geol. Soc. Am. Spec.  
881 Pap. 180, 177–194. 882
- Wohletz, K.H., Sheridan, M.F., 1983. Hydrovolcanic explosions II. Evolution of basaltic  
883 tuff rings and tuff cones. Am. J. Sci. 283, 385–413. 884
- Yamamoto, T., Nakamura, Y., Glicken, H., 1999. Pyroclastic density current from the 1888  
885 phreatic eruption of Bandai volcano, NE Japan. J. Volcanol. Geotherm. Res. 90,  
886 191–207. 887
- Yamaoka, K., Kawamura, M., Kimata, F., Fujii, N., Kudo, T., 2005. Dike intrusion associated  
888 with the 2000 eruption of Miyakejima Volcano, Japan. Bull. Volcanol. 67, 231–242. 889

890

# Phreatomagmatic volcanic hazards where rift systems meet the sea, a study from Ambae Island, Vanuatu

Nemeth K

2009